

Thermodynamic fluctuations of site energies and occupation numbers in the two-dimensional Coulomb glass

D. Menashe, O. Biham, and B. D. Laikhtman

Racah Institute of Physics, Hebrew University, Jerusalem 91904, Israel

A. L. Efros

Department of Physics, University of Utah, Salt Lake City, Utah 84112

(Received 2 August 2000; revised manuscript received 19 January 2001; published 31 August 2001)

The equilibrium thermodynamic fluctuations of site energies and site occupation numbers in a disordered two-dimensional system of localized classical interacting electrons, known as the Coulomb glass, are studied. Using computer simulations, it is shown that the configuration of occupied sites within the Coulomb gap persistently changes with time, even at temperatures much lower than the Coulomb gap width. A related effect is the fluctuations in the site energies, which are much larger than the temperature, and are of the order of the Coulomb gap width. Numerical arguments are presented that no thermodynamic glass phase transition occurs above $T=0$, so that at long enough timescales the system will always be in thermal equilibrium. The strong fluctuations in the occupation numbers and site energies are interpreted in terms of a drift of the system within the complex structure of phase space, which is characteristic of glassy systems. Such a drift could provide a new mechanism of electron diffusion, as long as the equilibration time of the system is short enough. However, in realistic systems with tunneling between sites there may be two different regimes. In the first regime the system is effectively frozen in one of the minima of phase space and the regular Efros-Shklovskii hopping is responsible for transport. Our results are applicable to the second regime where the localization length is $\xi \gg 1/T$. This may shine light on the issue of a possible metal-insulator transition in 2D systems.

DOI: 10.1103/PhysRevB.64.115209

PACS number(s): 72.20.Ee, 64.70.Pf, 75.10.Nr

I. INTRODUCTION

The role of electron-electron interactions in strongly disordered localized electron systems has long been an active area of research, following the pioneering papers by Pollak and Srinivasan.¹ While much still remains controversial, particularly regarding the relevance of interactions to transport,²⁻⁵ it is generally accepted that interactions play an important role in such systems. Of particular importance is the fact that the long range Coulomb interaction is not effectively screened at large distances, thus leading to the so-called Coulomb gap in the density of single particle states (DS) near the Fermi level.²

Another important effect of interactions is that the phase space of the many particle system has a so-called pseudo-ground state (PS) structure, first described by Baranovskii *et al.*,⁶ and recently studied⁷⁻⁹ in connection with slow relaxation times. These PS's are similar in nature to the local energy minima of glassy systems. In fact the analogy between the electron system and spin glasses was pointed out by Davies *et al.*¹⁰ in the early 1980's using different arguments. Subsequently, the term "Coulomb glass" or "Electron glass" has become widely used to describe interacting, strongly disordered electron systems. Recently, experimental confirmation of this analogy has been obtained through the observation of glassy dynamics in electron systems.^{11,12}

In this paper we study the thermodynamic properties of the two-dimensional (2D) classical Coulomb glass using Monte Carlo simulations. Our main observation is that the configuration of occupied sites within the Coulomb gap changes with time, even though the shape of the gap itself is time independent. This persistent change of the configuration

of occupied sites occurs even at temperatures which are much lower than the Coulomb gap width. A related effect is the fluctuations in the site energies, the magnitude of which is much larger than the temperature.

It is important that all these results do not follow from the picture of elementary excitation and diffusion in such a system proposed in Ref. 2. Consider the soft "pair" excitations which are close pairs of occupied and vacant sites. The excitation itself is a transition of the electron from one site to the other. They create a dipole potential which change the energy of nearest site by the energy I of the nearest neighbor interaction. However the relative fraction of such soft excitations is T/A , where A is the energy of disorder. Thus at $I \approx A$ the average magnitude of the displacement in the energy space is of the order of T . We show below that at large A the situation is similar. Compact many electron excitations give the same result because they are also dipole excitations and their number is also proportional to T . The excitations with large distance between vacant and occupied sites give even less displacement because their number is proportional to T^2 due to the Coulomb gap, even if they are combined with the compact excitations.

Thus, we have done a completely new observation which requires a new explanation. To interpret these results we note that while the various PS's are low in energy, they have very different sets of occupation numbers.

To get a very rough idea about PS consider the Wigner crystal on a square lattice with filling factor 1/2. In fact there are two states with the same energy and completely different occupation numbers. The meaning of PS in disordered system can be very roughly understood as the Wigner crystal with defects.

Thus, as the system drifts from one PS to another while in thermal equilibrium, many electrons are transferred between different sites, giving rise to the large fluctuations we observe. Since the energy distances between PS's are small this motion persists up to a very low temperature if the system is in equilibrium. The distances between PS's sharply decrease with the reciprocal size of the system.⁷ Unfortunately, the exact law is unknown. The thermodynamic fluctuations of energy that provide the change of the PS's are of the order of $T \cdot L$, where L is a linear size of the 2D sample. Then the motion should persist up to zero temperature for the infinite system. As we show below the time, that is necessary to see these fluctuations, increases exponentially with decreasing temperature, but this time is size independent. This is the basis of the new mechanism which we propose.¹³

A crucial ingredient of the above picture is the assumption that there is no finite temperature thermodynamic glass transition in the system. In the thermodynamic limit, such a transition would prevent the system from reaching thermal equilibrium below the transition temperature, thus limiting the validity of our results to finite size samples. In fact, no such transition has been observed either experimentally or numerically in the 2D Coulomb glass. Furthermore, this system has much in common with various 2D spin glass models, where there is strong numerical evidence that no finite temperature thermodynamic transition occurs.^{14,15} In the current work we present results which support such a conclusion for the 2D Coulomb glass as well. In Sec. IV D we show that for all available low temperatures there is a critical size of the system L_c , such that the equilibration time is independent of L at $L > L_c$. Both the equilibration time and L_c increase with decreasing temperature. One can also show that $L_c \approx 1/T$. This suggests the existence of the glass transition at $T=0$ as in the case of 2D spin-glass system.

Since the standard Coulomb glass Hamiltonian itself does not contain any dynamics, we employ dynamics which differ from the physical dynamics of a typical system, but are significantly faster. Namely, we assume that the hopping probability is independent of a distance between sites. Therefore, nonequilibrium phenomena, and particularly transport, cannot be studied directly by the methods discussed here.

However, the results of our work may have important implications for transport nonetheless. The size of a sample L plays the role of the maximum hopping length in our simulation. Speaking about a real system with the localization radius ξ one can think that L in our simulations is an analog of ξ in the real system. Since our simulation shows equilibration at $L > 1/T$, one can conclude that in the real infinite system it appears at $\xi > 1/T$. Thus, our results are applicable to the real system at $\xi > 1/T$. At smaller T the system is frozen in one of the PS and the transport mechanism should be Efros-Shklovskii (ES) hopping. Note that the exponent in the ES hopping becomes of order of one at $\xi T \approx 1$. The freezing of the system into one PS can be considered as a kinetic transition.

Thus, our results are especially significant near the insulator-metal transition, where the localization length is large and transitions between different PS's are fast. In such a case it is reasonable to expect that the fluctuations we have

described become more and more relevant, even to the point where they may change the nature of transport.

In fact, it has been demonstrated both for pure systems¹⁶ and systems with disorder,¹⁷ that such fluctuations may change the mechanism of the conductivity from percolation to diffusion because the random potential is time dependent. Thus, a connection may exist between glassy dynamics and the metal insulator transition, especially in 2D systems (See also Ref. 18).

The paper is organized as follows. In Sec. II we present the Hamiltonian of the Coulomb glass and derive two exact theorems connected with this Hamiltonian. Both of them are applicable in the thermal equilibrium and they serve as criteria of the equilibrium. One of them show that average occupation numbers are given by the Fermi function which is very unusual for a system with interaction. In Sec. III the computer simulations are described in detail. The results of the simulations and their interpretation are presented in Sec. IV and a summary in Sec. V. In this section we also discuss experiments on two-dimensional insulator metal transition in connection with our results.

II. THE HAMILTONIAN AND SOME EXACT PROPERTIES

For the purpose of our study we use the standard Coulomb glass Hamiltonian² given by

$$H = \sum_i \phi_i n_i + \frac{1}{2} \sum_{i \neq j} \frac{e^2}{r_{ij}} (n_i - \nu)(n_j - \nu). \quad (1)$$

The electrons occupy sites on a 2D lattice, $n_i = 0, 1$ are the occupation numbers of these sites and r_{ij} is the distance between sites i and j . The quenched random site energies ϕ_i are distributed uniformly within an interval $[-A, A]$. To make the system neutral each site has a positive background charge νe , where ν is the average occupation number, i.e., the filling factor of the lattice. In the current work we assume electron-hole symmetry, so that we only consider the case of half filling $\nu = 1/2$.

Hereafter we take the lattice constant a to be our length unit and e^2/a as our energy unit. Using these units, the single particle energy at site i is given by

$$\epsilon_i = \phi_i + \sum_j \frac{1}{r_{ij}} (n_j - \nu). \quad (2)$$

The Coulomb gap in the DS around the Fermi level of strongly disordered interacting electron systems has been studied extensively.^{2,6,10,19,20} In the 2D case at zero temperature, the DS near the Fermi level is linear in energy and obeys the mean field law

$$D(\epsilon) = \frac{2}{\pi} |\epsilon| \quad (3)$$

at $A \gg 1$, while the width of the gap is of the order of $E_g \sim 1/A$.^{21,22} As the temperature increases the gap is smeared at energies smaller than the temperature.^{10,23} It was shown²¹ that the case $A = 1$ can be considered as representative of

large A behavior since substantial deviation from the law Eq. (3) appears only at very low energy.

Another important result for the Coulomb glass Hamiltonian is that the average occupation number of a site with energy ϵ is given by the Fermi function. This result was obtained from an approximate self-consistent equation,²⁴ although it has been noted that an exact proof is possible.²¹ Due to the strong electron-electron interaction this is not at all obvious, and we thus provide this proof here. The average occupation number of sites with energy ϵ can be calculated by considering a single site $i=1$ and calculating its average

occupation number $\langle n_1 \rangle$ subject to the constraint that it has the required energy ϵ . By definition, this is given by

$$\langle n_1 \rangle = \frac{\text{Tr}\{n_1 \exp[-(H - \mu \sum_i n_i)/T] \delta(\epsilon - \epsilon_1)\}}{\text{Tr}\{\exp[-(H - \mu \sum_i n_i)/T] \delta(\epsilon - \epsilon_1)\}} \quad (4)$$

Here μ is the chemical potential. Note that $\mu=0$ at $\nu=1/2$ due to electron-hole symmetry. The Hamiltonian given by Eq. (1) can be written in the form $H = n_1 \epsilon_1 + H'$, where H' does not depend on n_1 . This enables us to separate out Tr_1 which is the trace over the variable $n_1=0,1$, thus obtaining

$$\langle n_1 \rangle = \frac{\text{Tr}_1\{n_1 \exp[-n_1(\epsilon - \mu)/T]\} \text{Tr}'\{\exp[-(H' - \mu \sum'_i n_i)/T] \delta(\epsilon - \epsilon_1)\}}{\text{Tr}_1\{\exp[-n_1(\epsilon - \mu)/T]\} \text{Tr}'\{\exp[-(H' - \mu \sum'_i n_i)/T] \delta(\epsilon - \epsilon_1)\}} = \frac{\text{Tr}_1\{n_1 \exp[-n_1(\epsilon - \mu)/T]\}}{\text{Tr}_1\{\exp[-n_1(\epsilon - \mu)/T]\}}. \quad (5)$$

Here Tr' and Σ' stand for the trace and sum over all n_i except n_1 . From Eq. (5) we readily obtain the Fermi function

$$\langle n_1 \rangle = f(\epsilon) \equiv \frac{1}{1 + \exp[(\epsilon - \mu)/T]}. \quad (6)$$

For the rest of the paper, the Fermi energy μ is taken as zero due to our assumption that the system is at half filling.

We thus find that at low temperatures a site changes its occupation number when its energy ϵ crosses the Fermi level. The site energy fluctuations described in Ref. 13 and elaborated on in Sec. IV B, mean that part of the sites in the system often change their occupancy, even at low temperatures. This leads to an interesting question regarding the distribution of average occupation number in the system. In the noninteracting case it is clear that as the temperature decreases, the average occupancy of most sites should be 0 or 1, and the probability to find a site with average occupancy near 1/2 decreases. However, in the interacting system the situation is much more complicated and the distribution of the average occupation number is nontrivial. We will now derive an analytic expression for the distribution of average occupation numbers $p(n)$, defined as the probability that a site will have time averaged occupancy n . This function is given by

$$p(n) = \overline{\delta(\langle n_1 \rangle - n)}, \quad (7)$$

where n_1 denotes the occupation number of (for example) the first site of the system, $\langle x \rangle$ denotes thermal averaging, and \bar{x} denotes disorder averaging. In the noninteracting case, the site energy just includes the random energy ϕ_1 , and is time independent, thus leading to $\langle n_1 \rangle = f(\phi_1)$. After performing the disorder average, the distribution of the average occupation number $p_0(n)$ in the noninteracting system is given by

$$p_0(n) = \frac{T}{2A} \frac{1}{n(1-n)} \Theta[e^{A/T}(n^{-1} - 1) - 1] \times \Theta[1 - e^{-A/T}(n^{-1} - 1)], \quad (8)$$

where Θ is the Heavyside step function. From Eq. (8) it is easy to see that as the temperature decreases, the distribution becomes sharply peaked around the values 0 and 1.

We now consider the interacting case. Referring to Eq. (7), we may write

$$p(n) = \frac{1}{(2A)^N} \int_{-A}^A d\phi_1 \cdots d\phi_N \delta\left(n - \frac{\text{Tr} n_1 \exp(-H/T)}{\text{Tr} \exp(-H/T)}\right), \quad (9)$$

where N is the number of sites, and H is the Hamiltonian given by Eq. (1). The Hamiltonian may be written as $H = n_1 \phi_1 + H'$, where H' does not depend on ϕ_1 , and then Eq. (9) takes the form

$$\begin{aligned} p(n) &= \frac{1}{(2A)^N} \int_{-A}^A d\phi_1 \cdots d\phi_N \delta\left(n - \frac{\sum_{n_1=0,1} n_1 \exp(-n_1 \phi_1/T) g(n_1, \phi_2, \dots, \phi_N)}{\sum_{n_1=0,1} \exp(-n_1 \phi_1/T) g(n_1, \phi_2, \dots, \phi_N)}\right) \\ &= \int_{-A}^A d\phi_1 \cdots d\phi_N \delta\left(n - \frac{\exp(-\phi_1/T) g(1, \phi_2, \dots, \phi_N)}{g(0, \phi_2, \dots, \phi_N) + \exp(-\phi_1/T) g(1, \phi_2, \dots, \phi_N)}\right) \\ &= \int_{-A}^A d\phi_1 \cdots d\phi_N \delta\left(n - \frac{1}{1 + \alpha(\phi_2, \dots, \phi_N) \exp(\phi_1/T)}\right), \end{aligned} \quad (10)$$

where $g(n_1, \phi_2, \dots, \phi_N) \equiv \text{Tr}' \exp(-H'/T)$, $\alpha \equiv g(0, \phi_2, \dots, \phi_N)/g(1, \phi_2, \dots, \phi_N)$, and Tr' signifies trace over n_2, \dots, n_N . Next we may perform the integration over ϕ_1 , which gives us

$$p(n) = \frac{1}{(2A)^N} \int_{-A}^A d\phi_2 \cdots d\phi_N \Theta[e^{A/T}(n^{-1}-1) - \alpha] \Theta[\alpha - e^{-A/T}(n^{-1}-1)] \frac{T[1 + \alpha \exp(\phi_1/T)]^2}{\alpha \exp(\phi_1/T)}$$

$$= \int_{-A}^A d\phi_2 \cdots d\phi_N \Theta[e^{A/T}(n^{-1}-1) - \alpha] \Theta[\alpha - e^{-A/T}(n^{-1}-1)] \frac{T}{[1 + \alpha \exp(\phi_1/T)]^{-1} \{1 - [1 + \alpha \exp(\phi_1/T)]^{-1}\}}, \quad (11)$$

where ϕ_1 is the solution to the equation $[1 + \alpha \exp(\phi_1/T)]^{-1} = n$, and $\Theta(x)$ is the step function. Note that for the sake of brevity we have dropped the arguments ϕ_2, \dots, ϕ_N from α . Using this definition for ϕ_1 , one immediately obtains

$$p(n) = \frac{T}{(2A)^N n(1-n)} \int_{-A}^A d\phi_2 \cdots d\phi_N \Theta$$

$$\times [e^{A/T}(n^{-1}-1) - \alpha] \Theta[\alpha - e^{-A/T}(n^{-1}-1)]. \quad (12)$$

Now, the integrand can take the values 0 or 1 and therefore, the final result may be written as

$$p(n) = \frac{T}{2A} \frac{1}{n(1-n)} \zeta(A, T, n), \quad (13)$$

where $0 < \zeta < 1$. Now, according to the definition of α given above, we may rewrite it as

$$\alpha = \exp(\Delta F/T), \quad (14)$$

where ΔF is the difference of the free energy of the Hamiltonian H' between configurations in which site 1 is occupied and unoccupied. Since this energy difference only contains the interaction energy between site 1 and all the other sites, it must satisfy $|\Delta F| \ll A$ for $A \gg 1$. This means that as long as $A \gg 1$, and as long as n is not too close to 0 or 1, one can put $\zeta = 1$ in Eq. (13). Therefore, under these conditions, we obtain the same result as in the noninteracting system. In Sec. IV B below we show that the numerical evaluation of $p(n)$ satisfies the noninteracting result [Eq. (8)] even for $A = 1$. This can be considered as further evidence that the case $A = 1$ is representative of systems with $A \gg 1$.

It is important to note that the results of Eqs. (6) and (13) were both obtained under the assumption that the system is in thermal equilibrium. This may be incorrect if there is a finite temperature glass transition and if the temperature is below the transition temperature. Thus, it is interesting to calculate these quantities numerically, and compare with the analytic results presented here. Such a comparison will be considered in Sec. IV B.

III. THE COMPUTATIONAL PROCEDURE

To study the equilibrium properties of the system we perform Monte Carlo (MC) simulations using the Metropolis algorithm. In our simulations we allow infinite range hopping, limited only by the system size. The hopping rate for an electron from an occupied to an unoccupied site does not depend on the distance between these sites but only on the energy difference between the initial and final configurations.

The use of such transition rates greatly decreases the equilibration time of the system compared to short range hopping transitions, and thus enables us to efficiently study the equilibrium behavior of the system. Once the system has reached thermal equilibrium, averaging over the simulation time is equivalent to ensemble averaging for the Hamiltonian of Eq. (1). However, the simulation time does not reflect the physical time in a Coulomb glass system, since the dynamics in the physical system is expected to be different. Related approaches are commonly used to study the thermodynamics of various spin glass models.²⁵ Note that the temporal behavior of nonequilibrium processes, such as transport properties, are expected to depend on the dynamics, and therefore cannot be studied using this approach.

The details of the simulations are as follows: The simulations are performed on a square lattice of $N = L \times L$ sites with periodic boundary conditions. In this torus geometry, the distance between two sites is taken as the length of the shortest path between them. Each site is assigned a random energy ϕ_i , according to the distribution described following Eq. (1). For the case of half filling ($\nu = 0.5$), $N/2$ electrons are distributed randomly amongst the N sites, and then the system is allowed to evolve according to the Metropolis dynamics. In each step we randomly select one occupied site and one unoccupied site. We then examine the move in which the electron in the occupied site hops to the unoccupied site and calculate the change $\Delta \epsilon$ in the total energy of the system due to this move. The MC attempt to perform this move is accepted with probability

$$p = \exp[-\max(0, \Delta \epsilon)/T], \quad (15)$$

or rejected with probability $1 - p$. After an accepted move is performed all the single site energies are updated accordingly. We define a single MC sweep as a series of N consecutive MC attempts (accepted or rejected). The MC time unit is then defined as the time elapsed during a single MC sweep.

Each one of the simulations presented below starts with an initial waiting period of t_w MC sweeps, in order to allow the system to reach thermal equilibrium. Only then we begin to perform measurements on the system at constant time intervals, until the simulation is terminated after t_{total} MC sweeps. We have taken t_w and t_{total} to be large enough so that all the results presented in this paper are independent of both.

We also take care to avoid size effects in our simulations. Two size effects are known for the Coulomb glass simulations.⁶ The first is Fermi energy fluctuations in a finite lattices with different disorder realizations, which are of the order of A/\sqrt{N} . In our simulation this effect is small. The other size effect is related to the Coulomb interaction. At zero temperature the DS of Eq. (3) is maintained by the possibility for an electron to hop a distance $r > 1/\epsilon$. In a finite lattice the hopping distance is limited by L which leads to a hard gap for $\epsilon < 1/L$. To avoid this we make sure that $T > 1/L$, which leads to temperature smearing of the size effect. In general, unless stated otherwise, the simulations were performed on a lattice of size $L=50$ for $T \geq 0.1$, and $L=100$ for $0.05 \leq T < 1$. We have found that these values of L are more than sufficient to ensure that all our results are L independent.

Finally, as with all simulations of this kind, the results need to be averaged over P different realizations of the random site energies $\{\phi_i\}$. Unless stated otherwise, the value $P=100$ was used throughout, since it was found that this provided for sufficient disorder averaging.

The measurements we perform on the system can be divided into two categories. The first category consists of *thermal averages*, where the measured quantity is averaged over the entire simulation. An example of this kind of measurement is the density of states (DS), where at each time interval we measure the distribution of site energies $D(\epsilon)$ and then calculate the thermal average $\langle D(\epsilon) \rangle$. The second category consists of *evolution measurements*, where we follow the evolution of a set of sites that were selected at some initial time, after the first t_w MC sweeps. An example of such a measurement is to choose at the initial time all the sites for which the single site energy [Eq. (2)] lies within a chosen range. The energy distribution of these sites is then extracted as a function of time in order to examine whether these sites remain in the same energy range or diffuse. The standard deviation of this energy distribution is then calculated and presented as a function of time.

IV. THE SIMULATION RESULTS AND DISCUSSION

A. Coulomb gap and distribution functions $n(\epsilon)$ and $p(n)$

In order to test our numerical procedure, we first studied the DS $\langle D(\epsilon) \rangle$ at different temperatures. Our results are shown in Fig. 1, where the Coulomb gap is clearly observed. The shape of the gap is consistent with previous results.^{10,19} The slope of the linear part of the curve is approximately $2/\pi$ in agreement with Eq. (3). In the inset of Fig. 1 we show the temperature dependence of $D(\epsilon=0)$, which appears to be linear in the temperature range studied.

As an additional test, we have calculated the time average of the site occupancy as a function of energy $\langle n(\epsilon) \rangle$. The

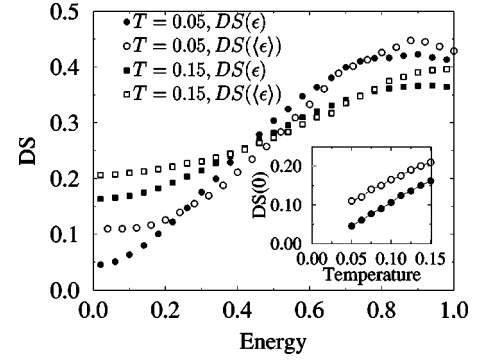


FIG. 1. The DS and the density of average site energies, for different temperatures and for $A=1$. Only positive energies are shown due to particle hole symmetry. Inset: the temperature dependence of the DS (solid marks) and the density of average energies (hollow marks).

results are shown in Fig. 2, where it can be seen that the curves are well fitted by the Fermi function.

In Fig. 3 we present the simulation results for the distribution of the average occupation numbers $p(n)$, defined by Eq. (7), together with the theoretical predictions which apply under equilibrium conditions. To generate this graph we calculate, for each site, the time averaged site occupancy $\langle n_i \rangle$ and then calculate the distribution function. The excellent agreement of $n(\epsilon)$ and $p(n)$ with theoretical expressions provides evidence that the system is in thermal equilibrium.

B. Spectral diffusion

We now turn to the central topic of this Section, which is the study of the thermodynamic fluctuations within the Coulomb gap. These fluctuations can be seen in a few ways. One is the time dependence of the single particle energies, which we call spectral diffusion.

To study the spectral diffusion, we first equilibrate the system during t_w MC sweeps. Then we mark all the sites whose single particle energies are in a narrow interval $[E_c$

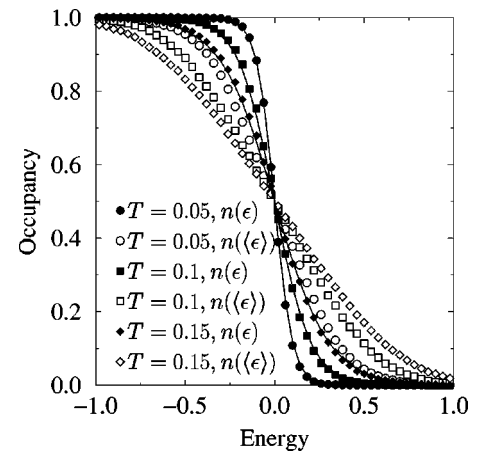


FIG. 2. Site occupancy as a function of site energy, and average site occupancy as a function of average site energy, for different temperatures and for $A=1$. The solid lines are the Fermi functions for the three shown temperatures.

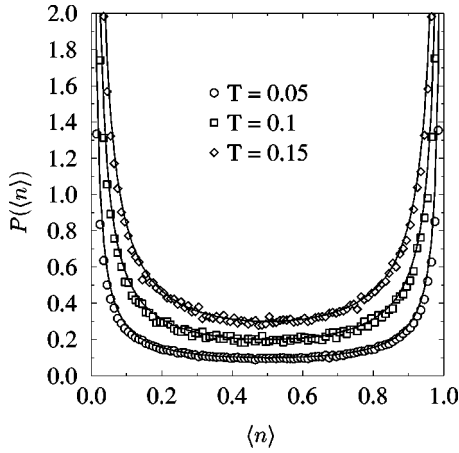


FIG. 3. Probability distribution of average site occupation numbers, for $A=1$ and different temperatures. The solid lines refer to the theoretical prediction, as discussed in Sec. II.

$-W, E_c + W]$ within the Coulomb gap as “test sites.” We follow the evolution of the distribution of these energies as the simulation proceeds. In Fig. 4 we present the standard deviation of this energy distribution $\delta\epsilon(t-t_w)$ as a function of time, for $E_c=0$, $W=0.05$, and different temperatures. As can be seen from the figure, after some number of MC sweeps, the standard deviation saturates. In the inset of Fig. 4 we plot the saturated value of the standard deviation as a function of temperature. Note that the temperature dependence is quite weak, and in all cases that standard deviation is much larger than the temperature. We have also checked that the DS of the test sites reaches an asymptotic form after the saturation time. This asymptotic form is shown in Fig. 5 for $E_c=0$, $W=0.05$, at two different temperatures. Note that the final energy distribution covers most of the Coulomb gap, although the initial distribution was centered in a small region at the center of the gap. This is in spite of the fact that the temperature is much smaller than the gap width. We have also studied the dependence of the final distribution on W , and have found that the results are independent of W for $W < 0.1$. Also shown in Fig. 5 is an example where the initial

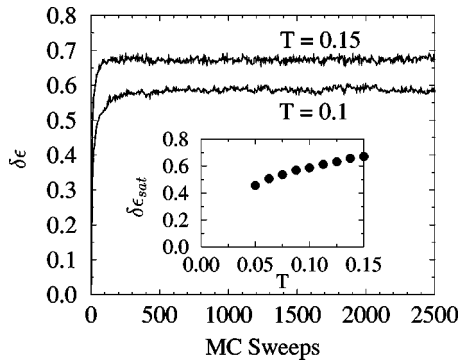


FIG. 4. The standard deviation, $\delta\epsilon$, of the distribution of test site energies, as a function of time, for $A=1$ and for three different temperatures. The test sites were chosen in the initial energy range $[-0.05, 0.05]$. Inset: the saturated value $\delta\epsilon_{\text{sat}}$ of the standard deviation as a function of temperature.

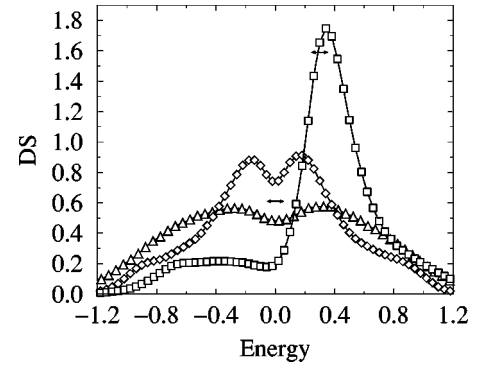


FIG. 5. Final energy distribution of sites initially in the energy range $[E_c - W, E_c + W]$. Diamonds (◇) are for $E_c=0$, $W=0.05$, $T=0.05$. Squares (□) are for $E_c=0.3$, $W=0.1$, $T=0.05$. Triangles (△) are for $T=0.1$, $E_c=0$ and $W=0.05$. The arrows mark the positions and widths of the two initial distributions of test sites which were used. All results are for $A=1$.

distribution is asymmetric, namely, $E_c \neq 0$. In this case, the asymptotic distribution is also asymmetric, however, it is nearly as broad as the symmetric distributions. Moreover, while the initial asymmetric distribution consists of only sites with positive energies (unoccupied sites), the final distribution also includes sites with negative energies (occupied sites).

Another way to observe spectral diffusion is to measure the time average of the single-particle energy at site i , $\langle \epsilon_i \rangle$, and the standard deviation at the same site, $\Delta_i = \sqrt{\langle \epsilon_i^2 \rangle - \langle \epsilon_i \rangle^2}$. We perform this calculation for all sites and create a function $\Delta(\langle \epsilon \rangle)$. This function is shown in Fig. 6 for $A=1$ and several temperatures. It is found that for all sites, the standard deviation of the single-particle energies is much larger than the temperature. Moreover, for sites with energies near the Fermi level the standard deviation is 2–3 times larger than for other sites.

We understand this picture in the following way. Sites with large Δ are expected to be “active” sites which change

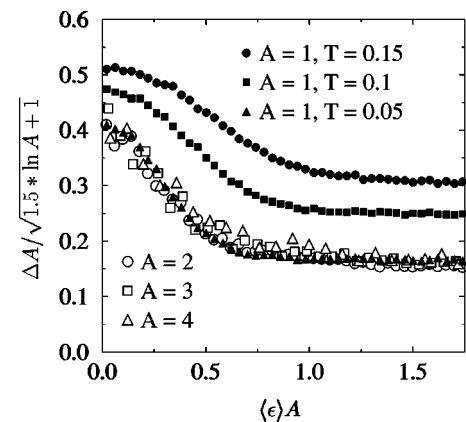


FIG. 6. Site energy standard deviation as a function of site average energy $\Delta(\langle \epsilon \rangle)$, for various values of A and T . For $A > 1$ the temperature is given by $T=0.05/A$, and we used a system size of $L=200$, and a number of disorder realizations $P=20$. Only possible energies are shown due to particle hole symmetry.

their occupation frequently as their energies cross the Fermi level. The changes in the occupation numbers of these sites are accompanied by a reorganization of the local configuration of occupied sites, which in turn is responsible for the larger value of Δ in a manner similar to the polaron effect. On the other hand, the sites with smaller Δ are “passive” sites, and change their energy only in response to the random time dependent potential created by the active sites. In the context of passive and active sites, it is instructive to define the quantity E_w as the energy at which $\Delta(\langle\epsilon\rangle)=\langle\epsilon\rangle$. The meaning of this is that sites which satisfy $\langle\epsilon\rangle < E_w$ have energy fluctuations larger than their average energy, and therefore are active. From Fig. 6 it is also apparent that these sites have larger value of Δ , thus supporting our understanding that these are indeed the active sites of the system.

The width of the maximum in Fig. 6 may indicate that the active sites are predominantly within the Coulomb gap. This is reasonable, since the occupation number of sites within the gap is strongly affected by interactions. However, at $A=1$ all characteristic energies, including the gap width, are of order unity. To check whether the active sites are indeed within the gap, we estimate the dependence of Δ on A for $A>1$ and compare it with simulations. The width of the gap E_g decreases with A as $E_g \sim 1/A$. The electron density within the gap is $n_g \sim \int_0^{1/A} \epsilon d\epsilon \sim 1/A^2$. If active sites make up a finite portion of all sites in the gap, they create a time dependent potential with the mean square value

$$\Delta^2 \sim n_g \int_1^A r^{-2} r dr \sim A^{-2} \ln A / A^2. \quad (16)$$

Here the logarithmic integral has been cutoff at the screening radius, which is proportional to the reciprocal density of states A .^{26,27} Note that this simple estimate does not take into account the polaron type effect mentioned earlier, and thus applies only to the random potential felt by passive sites. We have performed simulations for $1 \leq A \leq 4$ and plotted the results of $\Delta A / \sqrt{a \ln A + 1}$ against $\langle\epsilon\rangle A$. The temperature for each value of A is $T=0.05/A$, keeping it constant in units of the gap width. If our hypothesis is correct we should be able to choose the parameter a in such a way that all curves collapse in one, at least for large energies where the passive sites reside. One can see from Fig. 6 that indeed such a collapse occurs for $a=1.5$.

The temperature dependence of the results of Fig. 6 is presented in Fig. 7. The curves marked Δ_{\max} and Δ_{\min} show the maximal and minimal values of the standard deviation $\Delta(\langle\epsilon\rangle)$ as a function of temperature. The curve marked E_w shows the width of the function $\Delta(\langle\epsilon\rangle)$, which was previously defined. All the quantities shown in Fig. 7 appear to be much larger than the temperature for the entire temperature range shown. Furthermore, it appears that both Δ_{\min} and Δ_{\max} may tend to a finite value as $T \rightarrow 0$. We do not mean that it happens at fixed size of an array. We suggest the arguments below that it may be the case if the temperature decreases with increasing arrays. Here we can only mention that our lowest temperature $T=0.05$ may be a characteristic temperature which is connected to the size of the array only. Thus, if one expects that the observed linear dependence

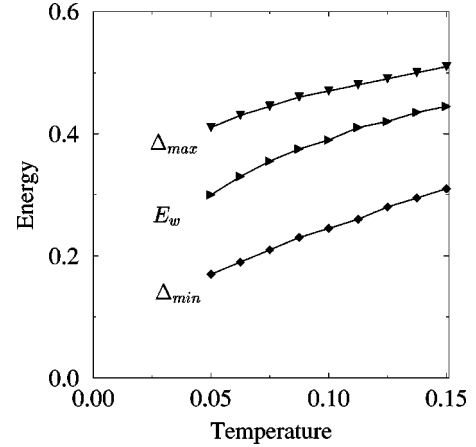


FIG. 7. Temperature dependence of quantities Δ_{\max} , Δ_{\min} and E_w for $A=1$. See text for a description of these quantities.

changes at lower T , so that all Δ tends to zero, this happens due to the finite size of the array.

Another manifestation of the spectral diffusion is a significant difference between the energy ϵ_i of a given site at a given moment and the time average of the energy of this site $\langle\epsilon_i\rangle$. To see this we compare the average occupation number $n(\epsilon)$ with the function $\langle n \rangle(\langle\epsilon\rangle)$. To generate $\langle n \rangle(\langle\epsilon\rangle)$ we first calculate the time averaged site occupancy $\langle n_i \rangle$ and the time averaged site energy $\langle \epsilon_i \rangle$ for each site. Then for all sites with given value of $\langle \epsilon_i \rangle$ we calculate the average value of $\langle n_i \rangle$. On the other hand $n(\epsilon)$ is obtained by averaging the occupation numbers of sites with the same energies at a given moment of time, and as we have seen both analytically and numerically, is just the Fermi function. In Fig. 2 we plot $\langle n \rangle(\langle\epsilon\rangle)$ together with $n(\epsilon)$, and one can see that for a given temperature $\langle n \rangle(\langle\epsilon\rangle)$ is not as steep as $n(\epsilon)$ near zero energy (the Fermi energy). This is due to $\langle n \rangle(\langle\epsilon\rangle)$ being smeared by energy fluctuations. For example, a site with $\langle \epsilon_i \rangle > 0$ may spend part of the time below the Fermi energy and, thus, enhance its occupancy.

Similarly, the distribution function of averaged energies, $D(\langle\epsilon\rangle)$ shown in Fig. 1, has a much less pronounced gap than $D(\epsilon)$. The reason is that the Coulomb gap exists for a distribution of site energies taken at the same moment of time. Due to fluctuations, $D(\langle\epsilon\rangle)$ is smeared because sites with small average energy $\langle\epsilon\rangle$ include sites which spend most of their time with larger energies, and thus have a higher density.

We understand the large energy fluctuation described above, and the large number of active sites implied by these fluctuations, as resulting from a drift of the system amongst the different PS's of phase space. Each PS is characterized by a unique set of sites forming the Coulomb gap. So that when the system drifts from one PS to another the number of sites that change their occupancy is a finite fraction of the number of sites in the Coulomb gap. As the temperature decreases, the fluctuations of the total system energy \sqrt{CT} (C being the heat capacitance of the system) decrease, and thus less PS's are accessible to the system. However, it has been shown⁷ that as the system size increases, the number of PS's increases, and the energy separation between them de-

increases. This means that at any given temperature, it is always possible to increase the system size so that there will be many PS's amongst which the system can drift. We believe this to be the source of the temperature independent contribution to the site energy fluctuations described above. For the finite systems sizes we use in our simulations, Δ will decrease to zero when \sqrt{CT} becomes smaller than the typical energy separation between PS's. In order to observe the temperature independent contribution to Δ at very low temperatures, it would be necessary to increase the system size beyond what is computationally feasible. However, we have taken care that there are no size effects for the temperature range presented in Fig. 7.

We believe that the temperature dependence that can be observed in Fig. 7 results from soft dipole excitations. These excitations are compact pairs of sites such that the energy change due to the transfer of an electron from one site of a pair to the other is very small.²⁸ The density of states of the dipole excitations is $1/A$, so that the concentration of active excitations is $\sim T/A$. These excitations not only contribute to the number of active sites, but also induce fluctuations of passive site energies, leading to the linear temperature dependence of Δ_{\min} observed in Fig. 7. Indeed, each dipole creates a potential r_0/r^2 at a passive site, where r is the distance between the site and the nearest dipole and $r_0 \sim 1/E_g \sim A$ is the size of the dipole.²⁸ Using the estimate above for the density of active dipole excitations, this leads to a slope of $\Delta_{\min}(T)$ close to that in Fig. 7.

C. Correlation function

Thus, the spectral diffusion shows that the configuration of occupied sites within the Coulomb gap persistently changes in thermodynamic equilibrium. To obtain more information about this motion, one can study the correlation function of occupation numbers. We do this by constructing a vector $\mathbf{D}(t_w)$ after t_w MC steps have been performed, whose components are the occupation numbers n_i of all sites within a given energy range $[-W, W]$. The vector is normalized so that $\mathbf{D}(t_w) \cdot \mathbf{D}(t_w) = 1$. As the simulation proceeds, we check the occupation number of these same sites, construct the vector $\mathbf{D}(t_w + t)$, and calculate the correlation function $C(t_w, t) = \mathbf{D}(t_w) \cdot \mathbf{D}(t_w + t)$. Correlation functions analogous to $C(t_w, t)$ are commonly used to measure the similarity between different configurations in systems such as spin glasses.¹⁵ For two identical configurations $C(t_w, t) = 1$, while if there is no correlation $C(t_w, t) = 0.5$. Basically, we are interested in $C_\infty = \lim_{t_w \rightarrow \infty} \lim_{t \rightarrow \infty} C(t_w, t)$, which is a measure of the similarity of two arbitrary states of the system at thermal equilibrium. For a noninteracting system,

$$C_\infty = \frac{\int_{-W}^W f^2(\phi) d\phi}{\int_{-W}^W f(\phi) d\phi}, \quad (17)$$

where $f(\phi)$ is the Fermi function. Thus, for the noninteracting system $C_\infty = 1 - T/W$ at $W \gg T$ and $C_\infty = 0.5$ at $T \gg W$.

In order to evaluate C_∞ from the simulation, we measure $C(t_w, t)$ as a function of t for a given t_w , and wait long enough so that $C(t_w, t)$ becomes independent of t . We denote

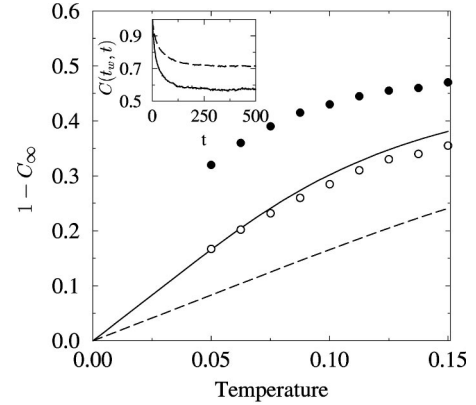


FIG. 8. The correlation function $1 - C_\infty$ as a function of temperature for $W=0.3$ (solid circles) and $W=0.6$ (open circles). Also shown are the theoretical curves for $1 - C_\infty$ in the case of a noninteracting system, for $W=0.3$ (solid line) and $W=0.6$ (dashed line). The inset shows $C(t_w, t)$ as a function of the time t , for $T=0.05$ (upper curve) and $T=0.1$ (lower curve). $A=1$ in all cases.

this saturated value as $C(t_w, \infty)$. In the inset of Fig. 8 we show an example of such a saturation. We then increase t_w until $C(t_w, \infty)$ becomes independent of t_w , and thus obtain our estimate of C_∞ .

The results for C_∞ for the interacting system are shown in the main part of Fig. 8 as a function of temperature, for $A=1$, $W=0.3$, and $W=0.6$. The corresponding functions for the noninteracting system, calculated directly from Eq. (17), are also shown. We observe that the correlation for the interacting system is much weaker than for the corresponding noninteracting system at the same temperature.

Note that by increasing W we include more sites in the correlation function C_∞ . However, our results for the spectral diffusion indicate that most of these additional sites remain passive as $T \rightarrow 0$. Thus, C_∞ should increase as W increases, as we indeed observe comparing the results for $W=0.6$ and $W=0.3$ (see Fig. 8).

The most interesting result coming from the study of the correlation function C_∞ is the possibility of a finite value for $\lim_{T \rightarrow 0} (1 - C_\infty)$. Clearly, such an extrapolation cannot be considered conclusive, however, one has to keep in mind the following points. First, while we have included in the definition of the correlation function only sites that were in the initial energy range $[-0.3, 0.3]$, it is clear that many passive sites are still included in this definition. These passive sites mask the behavior of the active sites and tend to increase the correlation. Second, a finite value of $\lim_{T \rightarrow 0} (1 - C_\infty)$ means that thermal motion continues down to zero temperature. This conclusion is consistent with the results obtained from the spectral diffusion in Sec. IV B and we understand it in the same way: Namely, we expect that a nonzero value of $1 - C_\infty$ may be obtained only if the size of the sample grows with the decrease of temperature so that \sqrt{CT} remains larger than the energy separation between different PS's.

It is important to point out that our results cannot be explained by assuming that the excitations of the system are separated pairs of sites, with electrons hopping back and

forth between the sites of each pair. This assumption would mean that electrons are effectively localized in space. Since the energy density of such excitations is constant at low energies, meaning the number of available excitations decreases linearly with temperature, one immediately obtains that $\lim_{T \rightarrow 0} (1 - C_\infty) \approx T/W$, as in the noninteracting system.

The same temperature dependence is obtained even if excitations involve a few electrons that change their positions simultaneously (so called many electron excitation^{29,1}). In fact, any picture based upon confined separated excitations which do not interact with each other would mean that $\lim_{T \rightarrow 0} (1 - C_\infty) \approx T/W$. Since our data definitely contradicts this temperature dependence, we conclude that such excitations cannot explain our results.

Thus, a nonzero value of $\lim_{T \rightarrow 0} (1 - C_\infty)$ can be explained only by a change of the electron configuration in the whole system, which cannot be broken into thermal motion confined to separate clusters. This means that there is a finite portion of electrons that are not localized in some region of space, but move around the whole system. We view this motion as another manifestation of the drift of the system amongst the different PS's of phase space.

D. The size dependence of the equilibration rate

An important question is whether the Hamiltonian of Eq. (1) exhibits a finite temperature glass transition in 2D. If so, then below the transition temperature the equilibration time should increase with system size L , and our results may also depend on L . Although all our results appear to saturate as a function of L , and we have presented evidence that the system is in thermal equilibrium for the temperatures studied, it would be instructive if we could directly study the size dependence of the equilibration time.

On the face of it this is not possible using the long range hopping dynamics presented in Sec. III, since we cannot derive from them the physical equilibration time of the system. However, the existence of a finite temperature glass transition in the system would mean that in the thermodynamic limit, it would not be possible to reach thermal equilibrium just using single particle excitations. Instead one would need to simultaneously move an infinite number of electrons to overcome the energy barriers. For finite size systems this would mean that the equilibration time (in units of MC sweeps), for any dynamics involving only single particle excitations, would grow with the system size. This would be true even if the hopping distance is infinite, as is the case here. To understand this point more thoroughly, it is instructive to use the standard analogy between the Coulomb glass and spin glasses.¹⁰ In this analogy, occupied and unoccupied sites are mapped to spin up and spin down, and an electron hop is equivalent to simultaneously flipping two spins. In the case of regular short range dynamics, the two spins would be close to each other, whereas in the case of long range dynamics the two spins may be located anywhere in the system. However, if a finite temperature glass transition existed, then the only way to overcome energy barriers in the thermodynamic limit would be to simultaneously flip an infinite num-

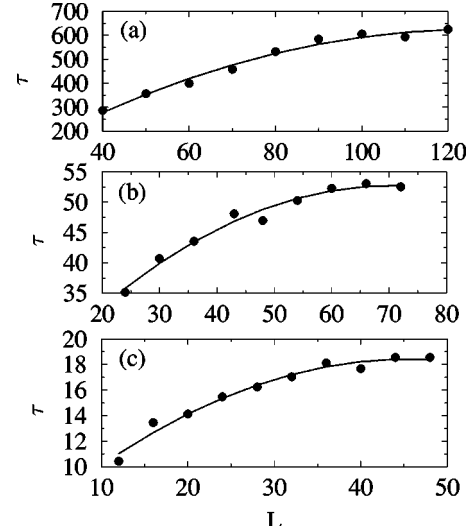


FIG. 9. The equilibration rate, τ (in MC sweeps), as a function of system size L , for $T=0.05$ (a), $T=0.1$ (b), and $T=0.15$ (c). The definition of the equilibration rate is given in Sec. IV D.

ber of spins. Specifically, one would not be able to reach thermal equilibrium by just flipping two spins each time, even if the distance between the two spins is allowed to be arbitrary.

For this reason we believe that if a finite temperature glass transition existed in the Coulomb glass with regular dynamics, it would also exist in the model studied here. To test this we have studied the size dependence of the equilibration rate of our model. The equilibration rate may be defined using a number of methods. The method we have chosen is to use the time dependence of the correlation function $C(t_w, t - t_w)$ defined in the previous subsection (An example of such a function is shown in the inset of Fig. 8). We have found that for any set of parameters, it is possible to fit this function with a stretched exponent of the form $C(t_w, t - t_w) = A \exp\{-[(t - t_w)/\tau]^\alpha\}$. While we do not necessarily attach any physical significance to the stretched exponential form, it enables to derive a time scale τ which we define as the equilibration time of system for the chosen set of parameters. As with all results presented in this paper, we take the waiting time t_w to be large enough so that τ is independent of t_w .

Our results are summarize in Fig. 9, where the equilibration time is plotted as a function of system size for three different temperature. All results are given for $A=1$. From these results it is clear that in the temperature range studied here, namely $T \geq 0.05$, the equilibration times saturate as a function of L . The value of L at which the equilibration times become L independent is the correlation length of the system, and from Fig. 9 it appears that it is inversely proportional to the temperature. In all our simulations we have taken care to ensure that the system size L is larger than the correlation length. The L -independent equilibration times strongly increases with decreasing temperature, making it difficult to study temperatures below $T=0.05$. However, since at $A=1$ the temperature $T=0.05$ is well below any relevant energy scale, we conclude that there is no finite temperature phase transition in the model studied here.

V. SUMMARY AND CONCLUSION

In this paper we have presented strong computational evidence that in a disordered 2D system of localized interacting electrons in thermal equilibrium, the configuration of occupied sites within the Coulomb gap persistently changes with time. This effect persists down to temperatures well below the Coulomb gap width, and it causes large temporal fluctuations of the site energies. The results are an exclusive property of the interacting system. Without interaction, only electrons in a small interval of width T would change their occupation, and the site energy fluctuations would be of order T .

We argue that this effect may exist in the limit $T \rightarrow 0$, as long as the sample size increases with decreasing temperature so that the energy separation between local minima of the total energy is much smaller than the thermal fluctuations of the total energy. We wish to emphasize that the results presented here are not sufficient to prove this point, and in fact such a proof is impossible using computational methods. Nevertheless, it is important to bear in mind that our simulations have been carried out at temperatures much lower than the Coulomb gap width, and thus cover the regime which is attainable by current experiments.

The strong fluctuations described in this work are a property of the Coulomb glass in thermal equilibrium. We have presented evidence that there is no finite temperature glass transition in the 2D Coulomb glass, and thus thermal equilibrium can be reached down to zero temperature. However, it is clear that as the temperature decreases, the equilibration time increases. This effect was observed in the long range hopping model studied here, and should be even more pronounced if more realistic short range hopping is used. At thermal equilibrium, namely, when the system has enough time to visit a macroscopically large portion of the PS's, there is a continuous rearrangement of the electronic configurations, possibly leading to a different conductivity mechanism. As the temperature is lowered, the system freezes into one PS for a long time, and this mechanism cannot compete with VRH transport. We believe this to be the reason for the well established experimental observation of VRH. At higher temperatures, the system equilibrates

faster, and the mechanism discussed above may dominate over VRH.

Thus, we believe that in a two-dimensional system there is a kinetic transition, from a frozen state to an equilibrium state. The paper by Levin *et al.*³⁰ gives a good confirmation of this point. In that paper all hops at a distance smaller than some length R have equal probability, while larger hops are forbidden. It has been shown that the conductivity behaves as $\exp[-\alpha/(RT)]$, where α is some constant. In fact, R plays here a role of the localization length ξ . One can think that kinetic transition appears when exponent is of the order of 1, which means that $\xi \approx 1/T$. We cannot observe this transition in our simulations since it is expected to depend on the physical kinetics and not only on the Hamiltonian. However, we may use the size effect on Fig. 9 to come to the same conclusion: there is no equilibration if the maximum tunneling length L is smaller than $\approx 1/T$.

The data by Kravchenko *et al.*³¹ supports the idea of such a kinetic transition. In this work it is shown that the resistivity of a 2D silicon layer with different electron densities collapses into two separate curves when plotted versus T/T_0 . The resistivity on the insulating side increases at low T according to $\exp(T_0/T)^{1/2}$. The resistivity on the metallic side decreases as the temperature is reduced. At $T > T_0$ both curves coincide and become temperature independent. For the insulating curve we consider T/T_0 as ξT (in our units), where ξ is the localization length. We believe that the temperature dependence of the insulating curve reflects the kinetic transition discussed above. Below T_0 the system is frozen in one local minimum and VRH transport dominates, leading to the exponential temperature dependence. Above T_0 the system equilibrates rapidly leading to temperature independent transport. The metallic conductivity at low temperature and higher density (metallic curve) cannot be understood in such a way.

ACKNOWLEDGMENTS

We are grateful to Z. Ovadyahu and A. Vaknin for many useful discussions. One of us (A.L.E.) is grateful to A. I. Larkin and B. I. Shklovskii for fruitful discussions. The work was funded by the US-Israel Binational Science Foundation Grant No. 9800097.

¹M. Pollak, *Discuss. Faraday Soc.* **50**, 13 (1970); M. Pollak, *Proc. R. Soc. London, Ser. A* **325**, 383 (1971); G. Srinivasan, *Phys. Rev. B* **4**, 2581 (1971).

²A.L. Efros and B.I. Shklovskii, *J. Phys. C* **8**, L49 (1975); A.L. Efros, *ibid.* **9**, 2021 (1976).

³M. Pollak and M. Ortuno, in *Electron-Electron Interaction in Disordered Systems*, edited by A.L. Efros and M. Pollak (North-Holland, Amsterdam, 1985).

⁴A. Perez-Garrido, M. Ortuno, E. Cuevas, J. Ruiz, and M. Pollak, *Phys. Rev. B* **55**, 8630 (1997).

⁵V.I. Kozub, S.D. Baranovskii, and I. Shlimak, *Solid State Commun.* **113**, 587 (2000).

⁶S.D. Baranovskii, B.L. Gelmont, B.I. Shklovskii, and A.L. Efros, *J. Phys. C* **12**, 1023 (1979).

⁷Sh. Kogan, *Phys. Rev. B* **57**, 9736 (1998).

⁸A. Diaz-Sanches, A. Möbius, M. Ortuno, A. Perez-Garrido, and M. Schreiber, *Phys. Status Solidi B* **205**, 17 (1998); A. Perez-Garrido, M. Ortuno, and A. Diaz-Sanches, *ibid.* **205**, 31 (1998)

⁹C.C. Yu, *Phys. Rev. Lett.* **82**, 4074 (1999).

¹⁰J.H. Davies, P.A. Lee, and T.M. Rice, *Phys. Rev. Lett.* **49**, 758 (1982); *Phys. Rev. B* **29**, 4260 (1984).

¹¹M. Ben-Chorin *et al.*, *Phys. Rev. B* **48**, 15 025 (1993); A. Vaknin and Z. Ovadyahu, *Phys. Rev. Lett.* **81**, 669 (1998); G. Martinez-Arizala *et al.*, *ibid.* **78**, 1130 (1997); C.J. Adkins *et al.*, *J. Phys. C* **17**, 4633 (1984).

¹²Z. Ovadyahu and M. Pollak, *Phys. Rev. Lett.* **79**, 459 (1997).

¹³E. Efros, D. Menashe, O. Biham, and B. Laikhtman, *Proceedings of the 8th International Conf. on Hopping and Related Phenom-*

- ena* [Phys. Status Solidi B **218**, 17 (2000)]; D. Menashe, O. Biham, B. Laikthman, and A.L. Efros, Europhys. Lett. **52**, 94 (2000).
- ¹⁴R.N. Bhatt and A.P. Young, Phys. Rev. B **37**, 5606 (1988).
- ¹⁵E. Marinari *et al.*, in *Spin Glasses and Random Fields*, edited by P. Young (World Scientific, Singapore 1998).
- ¹⁶A.L. Efros, Phys. Rev. Lett. **68**, 2208 (1992).
- ¹⁷D. N. Tsiganov and A. L. Efros, Phys. Rev. B **63**, 132301 (2001).
- ¹⁸A.A. Pastor and V. Dobrosavljevic, Phys. Rev. Lett. **83**, 4642 (1999).
- ¹⁹B. L. Shklovskii and A. L. Efros, *Electron Properties of Doped Semiconductors* (Springer, Berlin, 1984).
- ²⁰S.R. Johnson and D.E. Khmel'nitskii, J. Phys. C **8**, 3363 (1996).
- ²¹F.G. Pikus and A.L. Efros Phys. Rev. Lett. **73**, 3014 (1994).
- ²²M.E. Raikh and A.L. Efros, Pis'ma Zh. Éksp. Teor Fiz. **45**, 225 (1987) [JETP Lett. **45**, 380 (1987)].
- ²³Previous computations, as well as the computations presented here, are inconsistent with any temperature independent smearing of the Coulomb gap due to the Coulomb interaction, proposed recently by Kozub *et al.* (Ref. 5).
- ²⁴A.A. Mogilyanskii and M.E. Raikh, Sov. Phys. JETP **68**, 1081 (1989).
- ²⁵K. Binder and D. W. Heerman, *Monte-Carlo Simulation in Statistical Physics* (Springer, Berlin, 1997).
- ²⁶T. Ando, A.B. Fowler, and F. Stern, Rev. Mod. Phys. **54**, 437 (1982).
- ²⁷Detailed study of a screening in a system with the Coulomb gap one can find in paper S.D. Baranovskii, B.I. Shklovskii, and A. L. Efros, Sov. Phys. JETP **60**, 1031 (1984).
- ²⁸A. L. Efros and B. I. Shklovskii, in *Electron - Electron Interactions in Disordered Systems*, edited by A. L. Efros and M. Pollak (North-Holland, Amsterdam, 1985), p. 409.
- ²⁹M.L. Knotek and M. Pollak, J. Non-Cryst. Solids **8-10**, 505 (1972); M.L. Knotek and M. Pollak, Phys. Rev. B **9**, 664 (1974).
- ³⁰E.I. Levin, V.L. Nguen, B.I. Shklovskii, and A.L. Efros, Sov. Phys. JETP **65**, 842 (1987).
- ³¹S.V. Kravchenko, W.E. Mason, G.E. Bowker, J.E. Furneaux, V.M. Pudalov, and M. D'Iorio, Phys. Rev. B **51**, 7038 (1995).